

# APPLICATION OF PRINCIPAL COMPONENT ANALYSIS IN THE EVALUATION OF OPTICAL DETAIL TRANSFER BEHAVIOR IN OFFSET PRINTING

Reinhard Tosch\*

Keywords: paper, contrast, quality, fiber

## Abstract

Optical detail transfer characteristics of a chosen paper type were determined on a printed line grid with graduated column width with the help of a computer-linked microdensitometer. Signal amplitude, signal-noise ratio and the contrast transfer function were calculated based on the established optical density distributions perpendicular to the line grid taken from 78 prints. As a result of locally occurring discrepancies on the printed paper areas as well as statistical measurement errors, reliable approximation of the measurement data based on spatial frequency was not possible through analytical functions.

Spectral break-down of the interference-ridden data through the application of principal component analysis enables the establishment of the relevant portion of information from the optical parameters. Through the extraction of the principal components, strikingly different contrast transfer behavior, based on spatial frequency, was found related to the direction of the paper fiber.

## 1. Introduction

In the analysis of measurement values resulting from the evaluation of the optical detail transfer properties of printing on paper one is often

---

\* Undinenweg 3, D 04277 Leipzig, Germany

confronted with a plethora of measurement data. Multivariable data of these types are usually evaluated graphically with the help of comparison with curves of optical detail transfer parameters, based on spatial frequency, which can vary through the use of different paper qualities or as a result of variable physical or chemical influences in the printing regime. For an efficient quantitative evaluation of these optical remission curves, it is desirable to derive or define variables with which clearly arranged and expressive representations of the transfer properties of paper can be achieved.

The image information is stored on to the paper by a placed toner application in the printing process. The result is a change in reflection in contrast to the unprinted paper surface. Because of the absorption of the printing toner by the paper fibers, a change in the optical properties takes place in the volume and on the surface of the printed paper. Light cast on it is reflected only partially by the paper surface. A certain portion of light penetrates into the volume of paper and is scattered by the paper fibers. This scattering process bears a complex character.

Reflected light from the areas not covered by toner consists of a diffuse and a directed portion as well as of an additional scatter portion which is due to the paper volume. A portion of the scattered light is once again caught by the areas covered with toner. The reflected portion of the printed as well as the unprinted areas of the paper give evidence of a characteristic dependency on spatial location as well as a dependency related to a spectral composition. In evaluating reproduction quality, the question arises as to how the contrast is transferred with varying spatial frequencies. With the aid of printed line grids with graduated column width, it seems thus very likely to capture optical properties with measurement apparatus and with them the fidelity of the detail transfer of the print in comparison to the original from low to high spatial frequency areas with the help of a microdensitometer functioning in the reflection. A decisive foundation for this is the fact that the image information in the print transferred to the paper from the original across the printing plate and the rubber sheet can be described analogously to the method of procedure in scientific photography<sup>1</sup> and in offset copying<sup>2</sup> as two dimensional space distribution of the optical remission density  $D$ . Perpendicular to the printed line grid, a typical optical remission density tendency results for each type of paper and corresponding to the specific printing conditions. From the maximums  $D_{\max}$  and minimums  $D_{\min}$  of the spatial frequency based optical density process, important quality parameters such as the signal amplitude  $S$ , the signal-noise-ratio SNR and the contrast transfer function CTF can be calculated immediately. The following compilation contains the corresponding formulas for the calculation of these optical variables<sup>3</sup>.

# Formulas for the Calculation of Optical Parameters for Paper

optical parameter    calculation formula

signal amplitude  $S$      $S = D_{\max} - D_{\min}$

standard deviation  $\sigma$   
(noise)

$$\sigma = \sqrt{\frac{\sum_{i=1}^N (D_i - \bar{D})^2}{N - 1}}$$

mean optical  
density  $\bar{D}$

$$\bar{D} = \frac{\sum_{i=1}^N D_i}{N}$$

Signal-Noise Ratio  
SNR

$$\text{SNR} = \frac{S}{\sigma}$$

Contrast Transfer Function  
CTF

$$\text{CTF} = \frac{D_{\max} - D_{\min}}{D_{\max} + D_{\min}}$$

The usual determination of variables for a compressed characterization of these transfer curves is linked to an analytical description of the measurement curves.

As a result of stochastically occurring incongruities caused by the paper itself, but which may just as well result from the color transfer process, the search remains fruitless for a function able to approximate the entire course of the measurement curve in many cases. Additionally, such functions generally approximate only chosen parts or a partial portion of the resulting measurement curves. *Principal Component Analysis* (PCA) offers a remedy to this unsatisfactory situation. This algebraic "unsupervised learning method"<sup>4</sup> permits the determination of the variability of the measurement curve groups on the basis of experimental data sets, while enabling the reduction of the dimensions of a measurement data sets to a minimum.

The goal of our investigations was to determine the signal amplitude, the signal-noise ratio, and the contrast transfer function based on spatial frequency with the help of a microdensitometer. This was to be achieved with test prints of uniform paper quality, printed on line grids with a graduated line spacing - not only parallel but also perpendicular to the paper fiber direction. A further aim was to extrapolate the so-called basis curves or principle components from the corresponding measurement sets by using principal component analysis. With the aid of these principal components, an analysis of the optical reproduction characteristics can be performed based on the direction of the paper fiber.

## 2. PCA

A method of multivariable statistics, *Principal Component Analysis* is otherwise known in mathematics and physics as principal axis transformation. The starting point is a data matrix  $\hat{X}$  with m-lines and p-columns. The number of lines in  $\hat{X}$  corresponds to the number of the objects tested and the number of columns is the same as the number of variables measured in the experiment. The p-accident variables  $\hat{X}_j$  possess a certain common multivariable distribution in the basic totality which does not have to be assumed as multinormal at first. The distribution may have a covariance matrix which is estimated through the sampling covariance matrix S. The basis of the non-standardized PCA is formed by the centering by element of the original matrix  $X_{ij}$ :

(1)

$$X_{ij} = \hat{X}_{ij} - \overline{\hat{X}}_j.$$

in which  $\overline{\hat{X}}_j$  represents the  $j^{\text{th}}$  average column value.

The centered variations  $X_{ij}$  are then used in the calculation. If one considers the p-variable vectors to be coordinate axes, then these axes span a p-dimensional area. A new coordinate system is sought whose p-axes are found by turning the coordinate system in the p-dimensional variable area<sup>5</sup>. This corresponds to a linear transformation of the variable  $X_{ij}$  according to

(2)

$$x = U \cdot y.$$

The endless variety of possibilities for the design of the principal components is reduced by the limitation that the components ought to represent a maximum of the entire characteristic variance. The first

principal component encompasses a maximum of the total variance of all typical characteristics; the second represents a maximum of the residual variance remaining after the extraction of the first component, and so on.

The PCA thus analyzes the totality of all characteristic variations. Complicated relationships between data are reduced to a simple form since they can be represented through a smaller number of orthogonal axes. The task of solving this problem is called an Eigenvalue problem in algebra.

For the Eigenvalue problem, the equation

$$(3) \quad \mathbf{S} \mathbf{U} = \mathbf{U} \mathbf{\Lambda}$$

is valid.

The quadratic and symmetric  $(p, p)$ - matrix  $\mathbf{S}$  results from the multiplication, performed from the left, of the transposed matrix  $\mathbf{X}'$  and  $\mathbf{X}$ :

$$(4) \quad \mathbf{S} = \mathbf{X}' \mathbf{X}.$$

$\mathbf{\Lambda}$  is the diagonal matrix of the Eigenvalues

$$(5) \quad \mathbf{\Lambda} = \begin{bmatrix} \lambda_1 & 0 & \dots & 0 \\ 0 & \lambda_2 & \dots & 0 \\ \cdot & \cdot & \dots & \cdot \\ 0 & 0 & \dots & \lambda_p \end{bmatrix}.$$

Along the diagonal from  $\mathbf{\Lambda}$ , the  $\lambda$ , are ordered according to size:

$$|\lambda_1| > |\lambda_2| > \dots > |\lambda_p|.$$

$\mathbf{U}$  signifies the Eigenvector matrix, the columns of which are formed by the linear independent Eigenvectors  $\mathbf{u}_1, \mathbf{u}_2, \dots, \mathbf{u}_p$ , which belong to the Eigenvalues  $\lambda_1, \lambda_2, \dots, \lambda_p$ . The Eigenvectors are complementarily orthogonal. If both sides of the equation (3) multiplied with  $\mathbf{U}$  from the right, then

$$(6) \quad \mathbf{U} \mathbf{U}' = \mathbf{E},$$

in which E represents the unity matrix,

$$(7) \quad \mathbf{S} = \mathbf{U} \mathbf{\Lambda} \mathbf{U}'.$$

Equation (7) may also be written in the form<sup>5</sup>:

$$(8) \quad \mathbf{S} = \mathbf{U} \mathbf{\Lambda}^{1/2} \mathbf{\Lambda}^{1/2} \mathbf{U}'.$$

If one sets

$$(9) \quad \mathbf{U} \mathbf{\Lambda}^{1/2} = \mathbf{L}$$

then the spectral break-down of S:

$$(10) \quad \mathbf{S} = \mathbf{L} \mathbf{L}'$$

follows from equation (7),  
or

$$(11) \quad \mathbf{S} = \lambda_1 u_1 u_1' + \lambda_2 u_2 u_2' + \dots + \lambda_p u_p u_p'.$$

The matrix S is thus able to be completely reconstructed ( $s = p$ ) or approximated ( $s < p$ ) as a product of two factors, namely of the matrix

$$(12) \quad \mathbf{L} = \mathbf{U} \mathbf{\Lambda}$$

and of its transposition

$$\mathbf{L}' = \mathbf{\Lambda} \mathbf{U}'.$$

Equation 10 is also called a factorization of the covariance matrix S. This operation is clear since the coefficients are so chosen that the operation breaks down<sup>5</sup> the complete characteristic variation in orthogonal manner into consecutive portions diminishing in size. As a homogenous equation system, equation (3) has exactly then a non-trivial solution  $u_j = 0$  whenever the coefficient determinants of the system diminish for every value from  $u_j$ :

$$(13) \quad |\mathbf{S} - \mathbf{\Lambda} \mathbf{E}| = 0.$$

The determinants of the Eigenvalue problem can be calculated, for example, through the iteration process developed by Hotelling. In the PCA, the observed variables  $x_i$  are represented as a function of a

smaller number of hypothetical variations, from the principal components  $z_i$  (principal components = PC).

The model is

$$(14) \quad \mathbf{x} = \mathbf{W} \mathbf{z}.$$

The  $i^{\text{th}}$  principal component  $z$  is received in observance of the fact that the variation of  $y_i$  is the  $i^{\text{th}}$  Eigenvalue  $\lambda_i$ .

If one extends equation (14) with  $\Lambda^{1/2}$  and observes equation (2), it follows that

$$(15) \quad \mathbf{x} = \mathbf{U} \Lambda^{1/2} \mathbf{z}$$

and

$$(16) \quad \mathbf{W} = \mathbf{U} \Lambda^{1/2}.$$

$z_i$  are the values of the principal components or loads, and the  $W_{ip}$  are the weights of the  $p^{\text{th}}$  components in the  $i^{\text{th}}$  variations. With the aid of the variation percent rate<sup>5</sup>

$$(17) \quad \eta = \frac{\lambda_i}{\sum_{i=1}^p \lambda_i} \cdot 100\% ,$$

the measurement data variability represented by the corresponding principal component can be determined.

### 3. Methods

For the offset printing tests<sup>6</sup>, a super-marathon-printing plate by *Howson Algraphy* was used. A chrome template with line grids with graduated column width<sup>7</sup> served as a copy in the copying process. The liquid solvent used in printing contained GRA-additives<sup>8,9</sup> of 0.1; 1.0 and 2.0% vol. With the non-ionic surfactant tergitol 15-S-12 of type N with a molecular weight of 728 and a HLB value of 6.5<sup>10</sup>. Three different pH values: pH 3.6, 5.2 and 8.6 were adjusted in the liquid solvent for each GRA concentration. MF offset newspaper paper 45 g/m<sup>2</sup> by *Oy Tampella Ab* was used as printing paper. The characteristics of this type of paper are described in endnote (9)<sup>9</sup>. The Finnish offset paper toner W 1 was used in all tests.

The offset printing tests with the pH value and GRA graduated concentration liquid were performed (figure 1) according to a uniform liquid management regime (see endnote (9)). In this, a liquid management level of "20", considered optimal, served as both the starting point and end of the printing process. At the beginning of the corresponding test run, the optimal liquid management was so set that the optical full tone density of  $D = 1.2$  was achieved. After the liquid management had been lowered from level "20" over level "10" down to zero (level "2"), i.e. after reaching the lubricating limit, a renewed 4 tier rise in the application of the liquid took place. The printing process closed with the liquid management level of "20" once again.

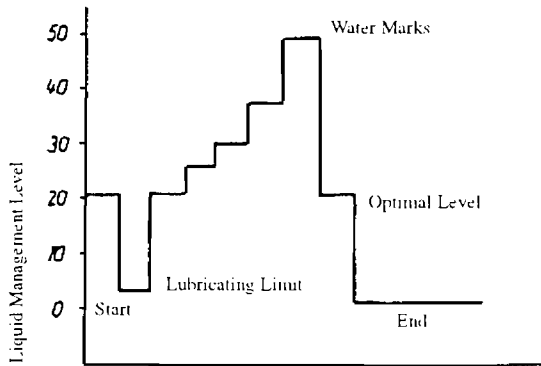


Figure 1 Schematic representation of the liquid management regime

## 4. Results

Measurement of the spatially dependent optical density tendency  $D$  took place by means of a microdensitometer connected to a computer and working in the reflection on line grids of graduated column width and parallel and perpendicular to the paper fiber direction on the 78 test prints; the printing quality was influenced by the texture of the paper as well as by the definitive chemical parameters of the fluid as the surfactant concentration and pH value, as well as the fluid management regime in addition. From this, the corresponding values were calculated for the signal amplitude  $S$ , the signal-noise ration SNR as well from the contrast transfer function CTF. The spatial frequency dependent average values of the corresponding optical parameter and the calculated loads  $z_i$  of the first three principal components established from the test prints are depicted in figures 2 to 7, as well as the related variance percent rate of the extrapolated principal components. While higher amounts in the average values of the signal amplitude as well as the values of the signal-noise ratio in contrast to the perpendicular measurement direction were found in the direction



of the paper fiber, the case of the contrast transfer function generated only small differences between both measurement directions.

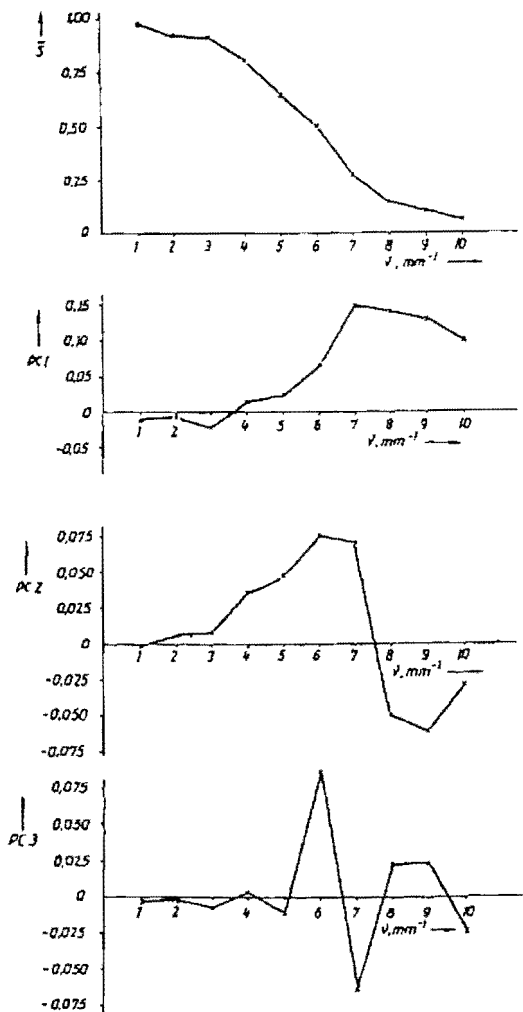


Figure 2 Average value of the spatial frequency dependent signal amplitude  $S$  of 78 test prints in the direction of the paper fiber with the corresponding loads of the first three principal components

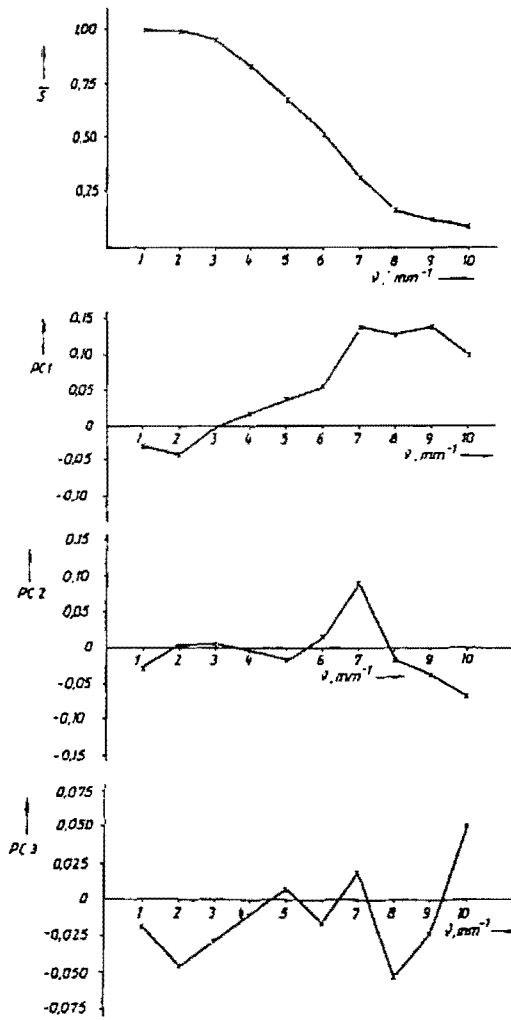


Figure 3 Average value of the spatial frequency dependent signal amplitude  $S$  of 78 test prints perpendicular to the direction of the paper fiber with the corresponding loads of the first three principal components

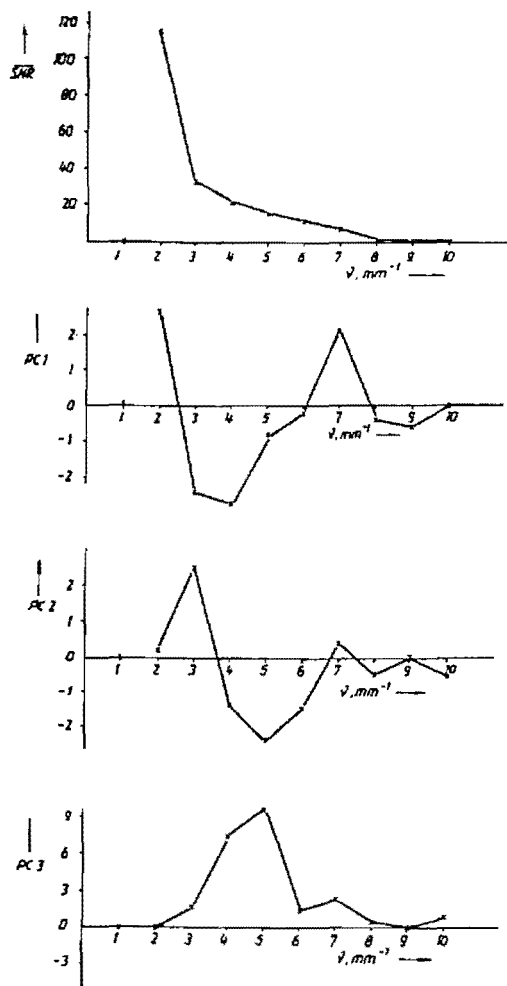


Figure 4 Average value of the spatial frequency dependent signal-noise ratio SNR of 78 test prints in the direction of the paper fiber with the corresponding loads of the first three principal components

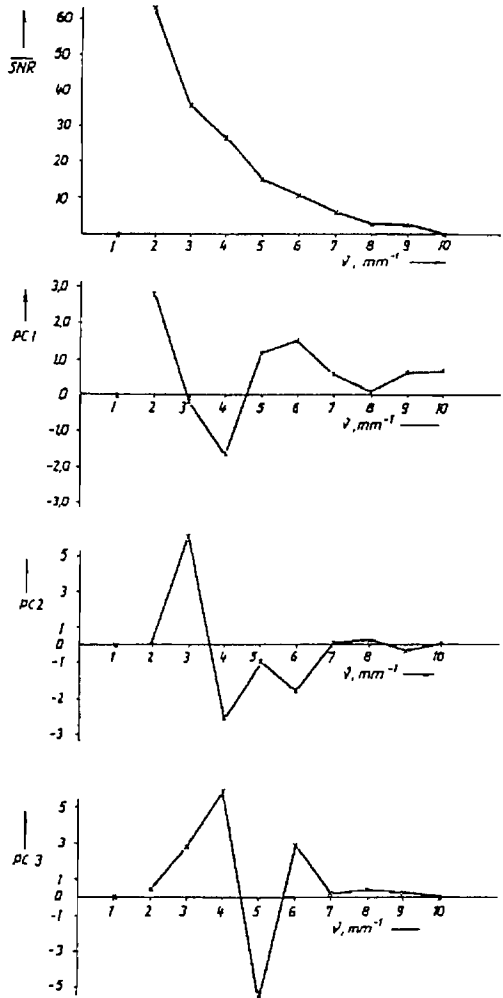


Figure 5 Average value of the spatial frequency dependent signal-noise ratio SNR of 78 test prints perpendicular to the direction of the paper fiber with the corresponding loads of the first three principal components

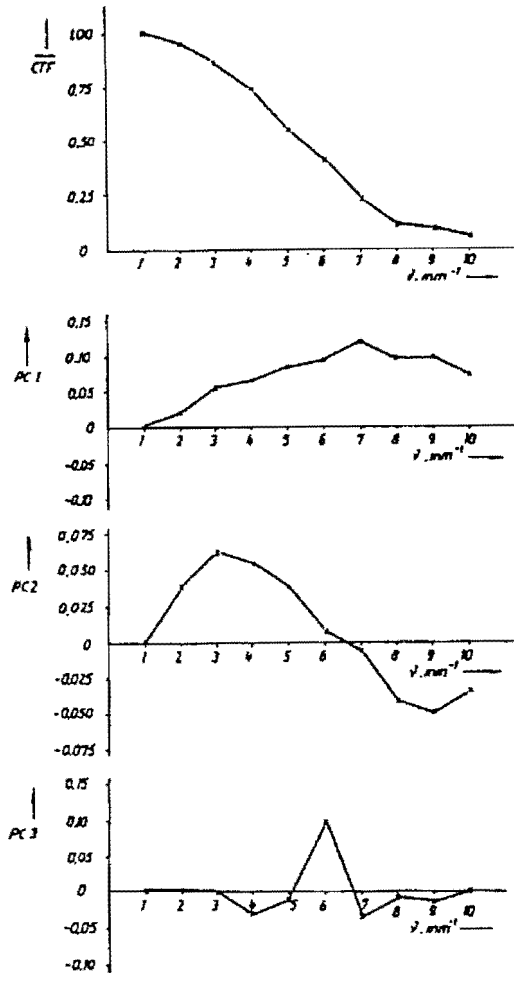


Figure 6 Average value of the spatial frequency dependent contrast transfer function CTF of 78 test prints in the direction of the paper fiber with the corresponding loads of the first three principal components

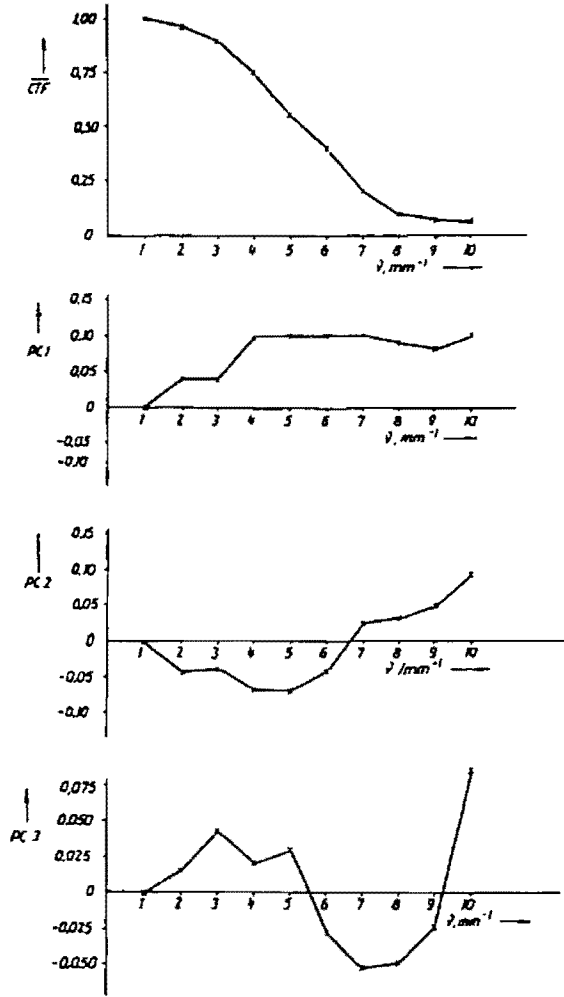


Figure 7 Average value of the spatial frequency dependent contrast transfer function CTF of 78 test prints perpendicular to the direction of the paper fiber with the corresponding loads of the first three principal components

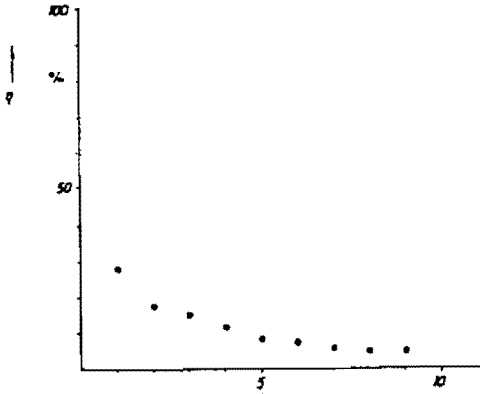
The result of the spectral break-down of the covariance matrices of the optical parameter data sets parallel to the direction of the paper fiber is a sharp contrast to those which were set perpendicular to it. It is noticeable that the contrast transfer function for both measurement directions of the other two tested parameters is characterized by the highest amounts in relation to the variance percent rate of the first three principal components (see figures 8 to 10). General consistency was established in the contrast transfer function as well as the signal amplitude in regard to the behavior of the load of the first principal component in amount and sign as opposed to the direction of the paper fiber. In contrast to this, strongly accented differences occur dependent on the measurement direction in the signal-noise ratio in this basis curve. Considerable variations from zero loads were detected in the second principal component in the direction of the paper fiber for the signal amplitude solely for the spatial frequency of  $\nu = 7 \text{ mm}^{-1}$  and  $\nu = 10 \text{ mm}^{-1}$ . In contrast to this, the loads of the second principal component demonstrate amounts clearly differing from zero perpendicular to this measurement direction in the spatial frequency interval of 4 to  $10 \text{ mm}^{-1}$ . Whereas with the signal-noise ratio, dominating differences manifest themselves in measurement variability in the different behavior of the first principal components, the direction of measurement has only a small influence on the loads of the second principal component. Other conditions exist in contrast transfer. In this case, a contrary behavior of the loads of the second main component was found in contrast to the first principal component in regards to the chosen direction of measurement on the paper. The loads of the second basis curve display a spatial frequency dependent, sine-like course in which a sign change of the loads from plus to minus occurs with increasing spatial frequency. Diametric to it, a basis curve was established in the direction of measurement perpendicular to the direction of the paper fiber. Both basis curves possess a joint path through zero and/ or a zero load at the spatial frequency of  $\nu = 7 \text{ mm}^{-1}$ . The characteristic sign for both measurement directions in the second basis curve corresponds with a change in the spatial frequency dependent contrast transfer behavior of the tests not only parallel but also perpendicular to the direction of the paper fiber. Since the  $2 \times 78$  CTF curves partially cut and even overlap, a graphical depiction of these curves has been omitted. While the CTF tends to fall in the direction of the paper fiber with low spatial frequency ( $\nu = 2$  to  $4 \text{ mm}^{-1}$ ), more level curve tendencies resulted in high spatial frequency areas in a majority of the cases. Inverse contrast transfer conditions were found perpendicular to the direction of the paper fiber. A change from level to steep curve tendencies could be read in a majority of cases here at the transition from low to high spatial frequencies in the CTF curves. In other words: fine details are contrasted better on paper in the direction of the fiber than perpendicular to the direction of the fiber. The overwhelmingly irregular occurrence of loads in the basis curves of a higher order

regarding the amount and sign reflects an increased presence of stochastic variables for both directions of measurement. However, this share of measurement value variability does not lend itself to interpretation.

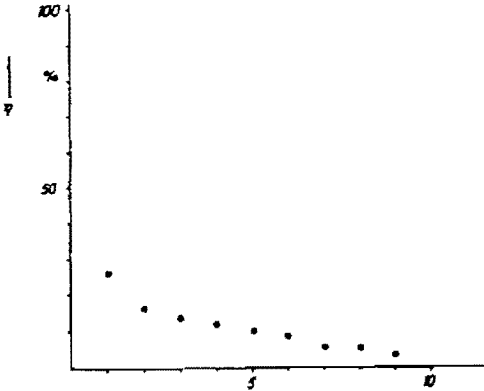
## Concluding Remarks

The detail transfer experiments parallel to the direction of the paper fiber and perpendicularly printed line grids of graduated column width contained the measurement of remission density courses with the help of a microdensitometer linked to a computer. Under the maintenance of one type of paper, printing conditions were varied regarding the fluid share, the pH value as well as the liquid management. The signal amplitude, the signal-noise ratio as well as the contrast transfer function were established in dependence on the spatial frequency from the measurement data density tendencies dependent on the spatial frequency. Finally, as a result of the unsatisfactory approximateability of the resulting measurement data through analytic functions, a characterization of the measurement value variability of these optical parameter data sets was performed by means of principal component analysis. A spectral break-down realized on this basis of the corresponding covariance matrices generated from the optical spatial frequency dependent parameter data sets resulted in a data compression which allowed an exact analysis of the influence of the direction of the paper fiber on the behavior of the optical parameter amplitude, signal-noise ratio as well as contrast transfer. With the extraction of both first principal components from the data sets of the spatial frequency dependent contrast transfer data, 70% of the total measurement value variability were able to be exhausted. In comparison to this, the measurement value variances of the data sets of signal amplitude based the spatial frequency and of the signal-noise ratio could be established only to about 55 and/or 42-45% by the first two principal components, whose ability to be characterized for both of these optical variables should be considered low.





Enumeration of the principal components in their order (measurement direction: perpendicular to the direction of the paper fiber)

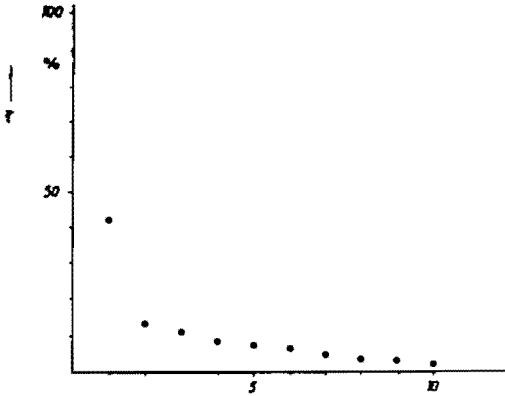


Enumeration of the principal components in their order (measurement direction: in the direction of the paper fiber)

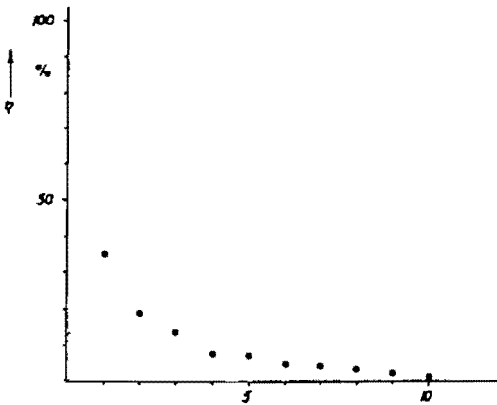
Figure 8 Variance percent rate for the 10 extrapolated principal components for the case of the spatial frequency dependent signal amplitude

From the mutual behavior of the second principal components, a dependency regarding the direction of the paper fiber was able to be proven in the case of the spatial frequency dependent contrast transfer. An explanation for this might be sought in a scatter behavior of the reflected light determined by the geometry of the paper fibers, which is connected to a direction dependent change of the capture of light by the printed paper areas. The examination of the spatial frequency dependent contrast transfer of printed paper also demonstrates that, as

a result of a removal of the noise-ridden portion from the optical data with the help of principal component analysis, important information hidden in the measurement data sets can be clearly and definitively identified, which otherwise would have been poorly or not at all recognizable by means of conventional analysis.

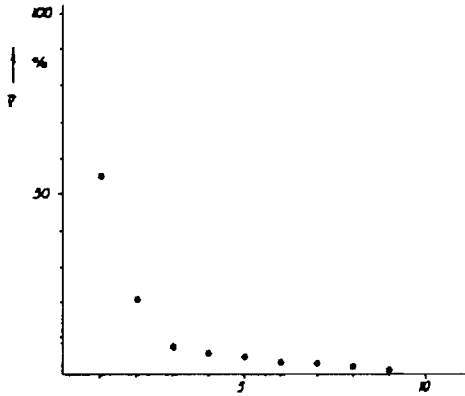


Enumeration of the principal components in their order (measurement direction: in the direction of the paper fiber)

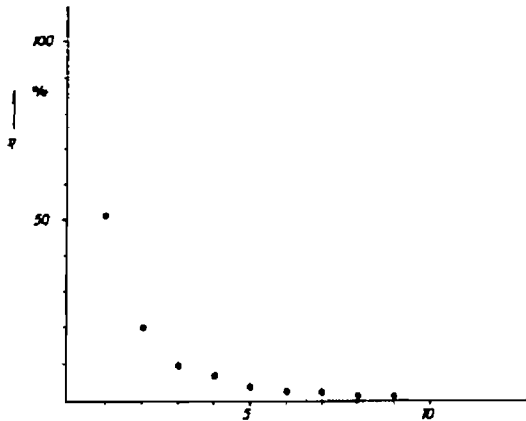


Enumeration of the principal components in their order (measurement direction: perpendicular to the direction of the paper fiber)

Figure 9 Variance percent rate for the 10 extrapolated principal components for the case of the spatial frequency dependent signal-noise ratio



Enumeration of the principal components in their order (measurement direction: in the direction of the paper fiber)



Enumeration of the principal components in their order (measurement direction: perpendicular to the direction of the paper fiber)

Figure 10 Variance percent rate for the 10 extrapolated principal components for the case of the spatial frequency dependent contrast transfer function

## Thanks

The author would like to express his gratitude to Dr. U. Lindqvist and J. Virtanen from the State Technical Research center of Finland, VTT, for their attentive care in performing the test prints. My thanks also go to Mr. K. Wolf, who was responsible for the assembly and testing of the computer-linked microdensitometer.

# Literature

- <sup>1</sup> Frieser, H.: Fotografische Informationsaufzeichnung. London: Focal Pr., 1975
- <sup>2</sup> Trauzeddel, R.; Tuovinen, P.; Wolf, K.; Tosch, R.: Sensitometric and copying Characteristics in Offset Platemaking. Graphic Arts in Finland 15 (1986), Nr. 2, 3-7
- <sup>3</sup> Jussila, E.; Oittinen, P.; Saarelma, H.; Tuovinen, P.: A System for Measuring Newspaper Print Quality. Graphic Arts in Finland 15 (1986), Nr. 2, 8-13
- <sup>4</sup> Hotelling, H.: Analysis of a Complex of Statistical Variables into Principal Components. J. Educational Psychology 24 (1933), Nr. 6, 417-433
- <sup>5</sup> Henrion, G.; Henrion, A.; Henrion, R.: Beispiele zur Datenanalyse mit BASIC-Programmen. Berlin: VEB Dt. Verl. D. Wiss., 1988
- <sup>6</sup> Virtanen, J.; Karttunen, A.; Traueddel, R.; Tosch, R.; Lindqvist, U.: Physio-Chemical and Electrostatic Characterization of Lithographic Systems. 20th. IARIGAI Conf. Moscow, Soviet Union, 1989
- <sup>7</sup> Jentsch, M.: Entwicklung und Erprobung einer Methode zur gleichzeitigen Bestimmung ausgewählter sensitometrischer und kopiertechnischer Kennzahlen vorbeschichteter Offsetdruckplatten. Leipzig, TH, Diss. A, 1983
- <sup>8</sup> Trauzeddel, R.; Tosch R.: Elektrokinetische Untersuchungen an Offsetdruckfarben. farbe + lack 95 (1989), Nr. 2, 105-108
- <sup>9</sup> Karttunen, A.; Lindqvist, U.; Virtanen, J.: Correlation Between Surface Chemical Properties of Lithographic Materials and their Behavior in Full Scale Printings. in: Bank, W.H.(Ed.): Advances in Printing Science and Technology. Proceedings of the 19th. IARIGAI Conf. Eisenstdt, Austria, 1987
- <sup>10</sup> Lindqvist, U.; Virtanen, J.: Surface and Interface Chemistry and Printing Characterization of Lithographic Materials. Internat. Conf. POLYGRAPH 88. Warsaw, 1988